ROVIBRATIONAL QUENCHING RATE COEFFICIENTS OF HD IN COLLISIONS WITH He

J. L. Nolte[1], P. C. Stancil[1], T.-G. Lee[2], N. Balakrishnan[3], AND R. C. Forrey[4]

[1] Department of Physics and Astronomy and Center for Simulational Physics, University of Georgia, Athens, GA 30602, USA;
jeffnolte@physast.uga.edu, stancil@physast.uga.edu
[2] Allison Physics Laboratory, Auburn University, Auburn, AL 36849, USA; tgl0002@auburn.edu
[3] Department of Chemistry, University of Nevada–Las Vegas, Las Vegas, NV 89154, USA; naduvala@unlv.nevada.edu
[4] Department of Physics, Penn State University, Berks Campus, Reading, PA 19610, USA; rcf6@psu.edu

ABSTRACT

Along with H_2, HD has been found to play an important role in the cooling of the primordial gas for the formation of the first stars and galaxies. It has also been observed in a variety of cool molecular astrophysical environments. The rate of cooling by HD molecules requires knowledge of collisional rate coefficients with the primary impactors, H, He, and H_2. To improve knowledge of the collisional properties of HD, we present rate coefficients for the He–HD collision system over a range of collision energies from 10^{-5} to $5 \times 10^3 \, \mathrm{cm}^{-1}$. Fully quantum mechanical scattering calculations were performed for initial HD rovibrational states of $j = 0$ and 1 for $v = 0$–17 which utilized accurate diatom rovibrational wave functions. Rate coefficients of all $\Delta v = 0$, -1, and -2 transitions are reported. Significant discrepancies with previous calculations, which adopted a small basis and harmonic HD wave functions for excited vibrational levels, were found for the highest previously considered vibrational state of $v = 3$. Applications of the He–HD rate coefficients in various astrophysical environments are briefly discussed.

Key words: early universe – ISM: molecules – molecular data – molecular processes – photon-dominated region (PDR)

Online-only material: color figures

1. INTRODUCTION

While H_2 has long been acknowledged as the main coolant in the primordial gas during the formation of the first baryonic objects, nevertheless the other primary coolant, HD, while less plentiful, may in certain circumstances play a comparable or even greater role in the cooling of molecular clouds to form the first stars. Although the HD/H_2 abundance ratio after freezeout is about 10^{-3} (Puy et al. 1993; Galli & Palla 1998; Stancil et al. 1998; Flower 2000), HD may contribute significantly relative to H_2 in cooling astrophysical media due to its permanent dipole moment—which allows transitions of $\Delta j = \pm 1$—and smaller rotational constant. The smaller spacing between energy levels and larger collisional rate coefficients allow for enhanced excited state populations and greater rates of energy transfer between the radiation field and matter (Flower 2000).

The relative importance of H_2 and HD in determining the thermal balance has been the subject of many studies. The question is important as stellar masses ultimately depend on the cooling properties of the dominant coolant in cloud collapse. Puy & Signore (1997) found that, for a $10^9 \, M_\odot$ protocloud, HD cooling would dominate at a matter temperature $T \sim 200 \, \mathrm{K}$ (close to the HD $j = 1 \rightarrow 0$ transition energy of 128 K), leading to a decrease in the matter temperature and possibly to cloud fragmentation. Similarly, Flower & Pineau des Fôrets (2001) showed that HD would contribute as much as 20% of the radiative cooling in post-shock gas. The contribution of HD to the heating of the gas when the radiation temperature exceeds the kinetic temperature was addressed by Flower (2000), who showed that the HD contribution could become comparable to H_2 at a redshift of $z \sim 25$. Likewise, Galli & Palla (1998) showed that HD dominates the heating of primordial gas at temperatures $\lesssim 150 \, \mathrm{K}$ in the low-density limit. More recently, Lipovka et al. (2005) used an updated HD cooling function to show that the HD cooling efficiency was significant even at high gas densities and temperatures, with the HD contribution comparable to that for H_2 at temperatures $\gtrsim 3000 \, \mathrm{K}$.

However, there is a question of whether the primordial gas can reach sufficiently low temperatures for HD cooling to dominate, and many early studies indicating an enhanced role of HD focused only on the beginning stages of cloud collapse. Nakamura & Umemura (2002a, 2002b) examined the conditions under which gas temperature becomes sufficiently low (~ 100–200 K) for HD to become the primary regulator of thermal evolution. They concluded that, under the conditions at which the first pregalactic objects are expected to collapse (namely, at $z \sim 10$–10^2 and masses of 10^5–$10^8 \, M_\odot$ in a cold dark matter cosmology), there will be an insufficient amount of H_2 to lower the temperature to the requisite values (contrary to the findings of Galli & Palla 2002), although HD cooling will sufficiently lower the gas temperature to produce fragment masses a few times smaller than without HD cooling. Moreover, they point out that HD may still play a dominant role in star formation in metal-deficient early galaxies, where gas photoionized by ultraviolet (UV) radiation favors the formation of sufficient amounts of H_2 to cool the gas below the threshold temperature, beyond which HD cooling controls the cloud fragmentation.

There may be other star formation scenarios in which the gas can become sufficiently cool for HD cooling to dominate. Uehara & Inutsuka (2000) investigated the role of HD cooling in the evolution of post-shock fragmentation. They concluded that HD cooling dominates for a shock velocity of $300 \, \mathrm{km \, s^{-1}}$ and leads to the formation of low-mass stars and possibly brown dwarfs. Fossil H II regions have also been identified as an environment in which HD may play a significant role. Nagakura & Omukai (2005) found that within initially ionized massive ($\gtrsim 10^6 \, M_\odot$) halos, HD cooling could lead to the formation of

low-mass stars. The possibility of HD-moderated formation of low-mass stars was also investigated by Machida et al. (2005) within the remnants of primordial supernovae. Simulations by McGreer & Bryan (2008) cast doubt on whether HD cooling in ionized halos would lead to formation of significantly lower mass stars, but showed that in low-mass ($\sim 10^5\ M_\odot$) unperturbed halos in which HD surpassed H_2 cooling, relatively low-mass stars (~ 6 times lower than without HD cooling) could form.

Of course, the accuracy of any model of protostellar collapse depends on the chemical data employed. Collisional rate coefficients are one fundamental ingredient in determining the thermal balance of the molecular gas and in this work we consider the quenching of HD excitation due to He collisions. For the He–HD system, the most recent calculation of rate coefficients for collisional rovibrational excitation was performed by Roueff & Zeippen (2000) in a fully quantal close-coupling approach using the He–H_2 potential surface of Muchnick & Russek (1994), hereafter referred to as the MR potential or potential energy surface (PES). Roueff & Zeippen reported rate coefficients for rovibrational transitions between the first 45 rovibrational levels of HD, with a maximum initial vibrational quantum number of 3. In this work, we extend their earlier calculations by computing all $\Delta v = 0, -1$ and -2 transitions for all initial states $v = 0$–17, $j = 0$–1, for temperatures $10^{-4}\ \mathrm{K} \leqslant T \leqslant 10^3\ \mathrm{K}$. Further, Roueff & Zeippen (2000) adopted the harmonic approximation for the HD vibrational wave functions, while the current computations utilize explicit, numerical diatomic wave functions obtained on an accurate molecular hydrogen interaction potential.

2. COMPUTATIONAL DETAILS

Inelastic He–HD cross sections were obtained using the nonreactive scattering program MOLSCAT developed by Hutson & Green (1994). In the close-coupling method employed here, the total wave function of the scattering system is expanded in terms of a basis set of Hermite polynomials. The resulting set of coupled differential equations in the expansion coefficients may then be solved and fitted to the appropriate form in the asymptotic region. The MR potential surface for He–H_2 was used, but with bond lengths scaled and the H–D center of mass along r shifted to account for the change in the D mass. This potential was the subject of a study by Lee et al. (2005), in which calculations of total He–H_2 quenching rate coefficients showed it to give better agreement with experimental data than the more recent potential of Boothroyd et al. (2003).

It is convenient to expand the atom–diatom interaction potential, $V(r, R, \theta)$, in terms of Legendre polynomials:

$$V(r, R, \theta) = \sum_{\lambda=0}^{\lambda_{\max}} v_\lambda(r, R) P_\lambda(\cos\theta), \qquad (1)$$

where r is the internuclear distance of HD, R is the distance of He from the diatom's center of mass, and θ is the angle between $\mathbf{r}$ and $\mathbf{R}$. The scattering equations then take the form (Flower 2007)

$$\left[\frac{d^2}{dR^2} - \frac{l(l+1)}{R^2} + k_{vj}^2 \right] F(vjlpJ|R)$$
$$= 2\mu \sum_{v'j'l'\lambda} f_\lambda(jl, j'l'J) y_\lambda(vj, v'j'|R) F(v'j'l'pJ|R), \quad (2)$$

where $k_{vj}^2 = 2\mu(E - \epsilon_{vj})$, E being the total energy, ϵ_{vj} the energy of the rovibrational state, and v, j, l, p, and J being

the vibrational, rotational angular momentum, orbital angular momentum, parity, and total angular momentum quantum numbers, respectively; $f_\lambda(jl, j'l'J)$ is a Percival–Seaton coefficient (Percival & Seaton 1957), and

$$y_\lambda(vj, v'j'|R) = \int_0^\infty \chi^*(vj|r) v_\lambda(r, R) \chi(v'j'|r) dr, \qquad (3)$$

with $\chi(vj|r)$ being the vibrational wave functions of HD. ϵ_{vj} and $\chi(vj|r)$ are obtained by solving the diatom nuclear Schrödinger equation with the H_2 potential of Schwenke (1988) and a basis of Hermite polynomials.

The cross sections are obtained from the scattering matrix S_J via

$$\sigma_{vj \to v'j'} = \frac{\pi}{k_{vj}^2 (2j+1)} \sum_{J=0}^{J_{\max}} \sum_{l=|J-j|}^{|J+j|}$$
$$\times \sum_{l'=|J-j'|}^{|J+j'|} (2J+1) |\delta_{vv'}\delta_{jj'}\delta_{ll'} - S_J(vjl, v'j'l')|^2. \quad (4)$$

Collisional rate coefficients are obtained by averaging the cross sections over a Boltzmann distribution of energies at a given temperature T:

$$k_{vj \to v'j'}(T) = \left(\frac{8}{\pi \mu k_b^3 T^3} \right)^{1/2}$$
$$\times \int_0^\infty \sigma_{vj \to v'j'}(E_{vj}) E_{vj} e^{-E_{vj}/(k_b T)} dE_{vj}, \quad (5)$$

where $E_{vj} = E - \epsilon_{vj}$ is the kinetic energy in the vj initial state.

The calculations employed a sizable basis set of at least 90 vj levels for each collision energy and initial rovibrational state. The basis states ranged over vibrational levels from at least $v - 3$ to $v + 1$. The potential expansion in each case included $\lambda_{\max} \geqslant 29$. Convergence was tested for all parameters, including the number of partial waves $l_{\max}$, the number of integration points, matching radius, basis set size, etc. For most calculations, convergence with respect to all parameters was ensured to within at least three significant figures, although in some cases, particularly for higher collision energies and initial vibrational numbers, a precision of only one or two significant figures was attained. In such cases, the reduction in precision applied mainly to cross sections for vibrationally inelastic $\Delta j = -2$ transitions which tend to be smaller.

3. RESULTS

Figures 1–3 show cross sections and rate coefficients for different families of Δv, Δj transitions over a large energy and temperature range. The data include the ultracold regime to demonstrate the effect of resonances near $0.1\ \mathrm{cm}^{-1}$ and the threshold behavior of the cross sections and rate coefficients as they approach the Wigner limit. The illustrated data are a small, but representative sampling of the entire set of calculations.[5]

Cross sections and rate coefficients for the dominant rotational quenching $\{v, j = 1\} \to \{v' = v, j' = 0\}$ family of

---

[5] All computed cross section and rate coefficient data can be obtained from the UGA Molecular Opacity Project database Web site:
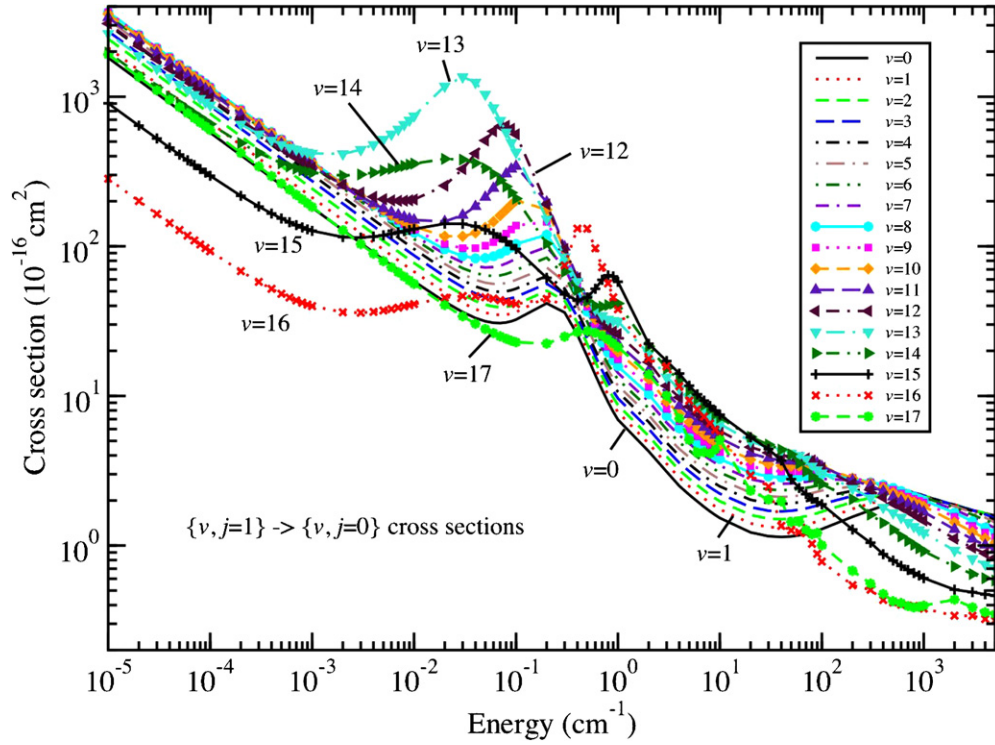http://www.physast.uga.edu/ugamop/

Figure 1. He–HD inelastic cross sections for $\{v, j = 1\} \rightarrow \{v' = v, j' = 0\}$.
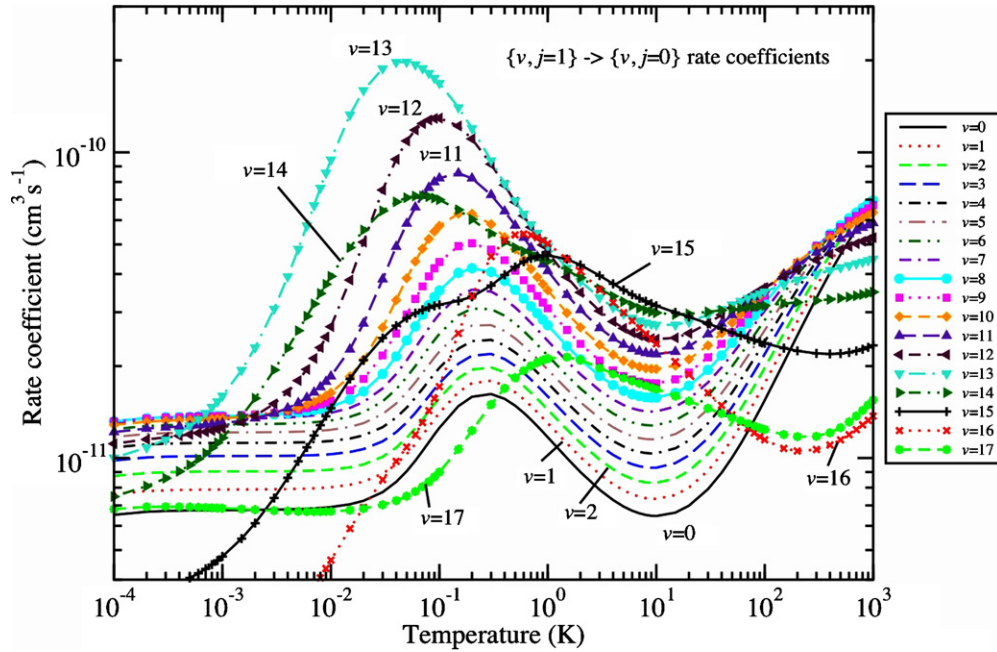(A color version of this figure is available in the online journal.)

Figure 2. He–HD inelastic rate coefficients for $\{v, j = 1\} \rightarrow \{v' = v, j' = 0\}$.
(A color version of this figure is available in the online journal.)

transitions are plotted in Figures 1 and 2, respectively. An orbiting resonance, which appears near $0.2\,\mathrm{cm}^{-1}$ in the cross section for $v = 0$, is seen to migrate to $0.03\,\mathrm{cm}^{-1}$ by $v = 13$ as shown in Figure 1. The resonance is responsible for the peak in the rate coefficients near 0.5 K in Figure 2, but also causes the increase in the rate coefficients for decreasing temperatures below $\sim$10 K. For most energies and temperatures, we generally find an increase in the cross section and rate coefficient with vibrational state v. In the range of about 1–10 K, for instance, we observe this trend for vibrational levels up to $v = 15$, with the rate coefficient decreasing slightly for $v = 16$, while for $v = 17$ it drops significantly. At lower v, this trend reflects the decreasing energy gap between the first two rotational states of a given vibrational level as v increases. However, at higher vibrational levels the diatom potential becomes increasingly anharmonic at large values of r, significantly affecting the y_λ term of Equation (3),
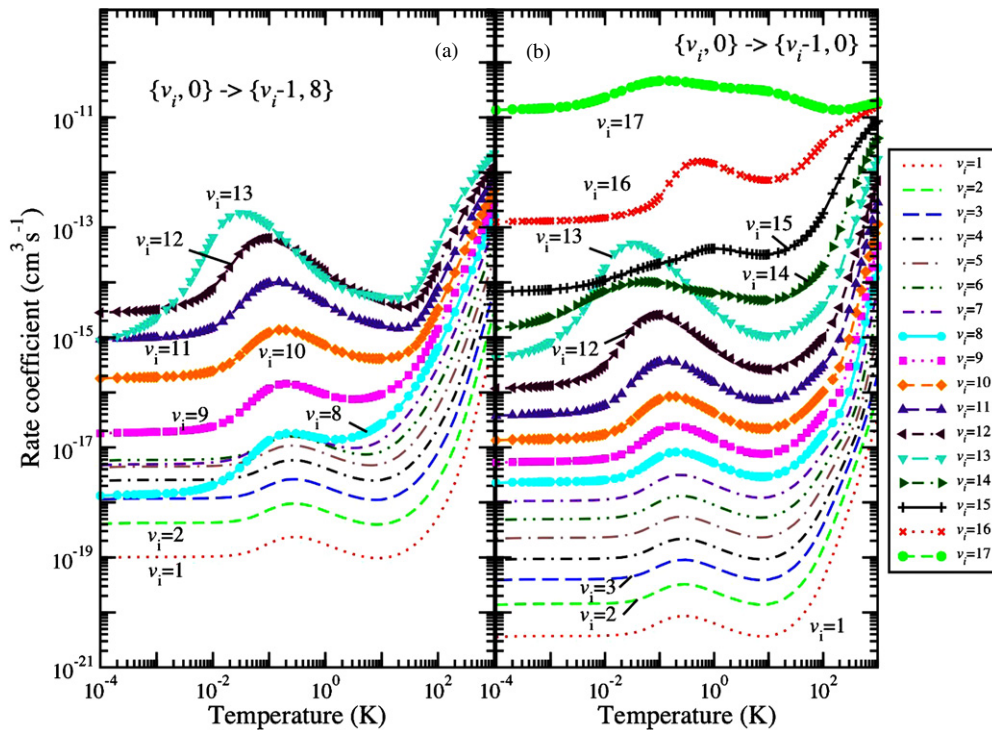
Figure 3. He–HD inelastic rate coefficients for (a) $\{v, j = 0\} \rightarrow \{v - 1, j' = 8\}$ and (b) $\{v, j = 0\} \rightarrow \{v - 1, j' = 0\}$.
(A color version of this figure is available in the online journal.)

accounting for the departure of $v = 16$ and 17 from the trend. Further, there is some uncertainty as to whether the $v = 17, j = 1$ level is bound. The HD dissociation energy has been measured by Zhang et al. (2004) to be $36405.828 \pm 0.16 \, \text{cm}^{-1}$, while experimental excitation energies are $36401.39 \, \text{cm}^{-1}$ for $v = 17$, $j = 0$ and $36406.10 \, \text{cm}^{-1}$ for $v = 17, j = 1$ (Dabrowski & Herzberg 1976). The $v = 17, j = 1$ level is thus very near dissociation which likely contributes to its marked departure from the overall trend. In the low-temperature limit, we again see rate coefficients increase and peak for $v = 8$, and then decrease for increasing v up to $v = 16$. This folding over in the neighborhood of the zero-energy resonance appears to reflect the changing energy of the least bound triatomic state for each initial rovibrational level.

Figure 3 shows two families of vibrational quenching rate coefficients, those of $\{v, j = 0\} \rightarrow \{v - 1, j' = 8\}$ and $\{v, j = 0\} \rightarrow \{v - 1, j' = 0\}$ transitions. Here again a general trend of increasing rate coefficients with increasing v is evident. However, the regular ordering is modified for higher vibrational states as the resonance near 0.5 K migrates to lower temperatures, vanishes, and is replaced by a higher temperature resonance. We note also that the rate coefficients are spread over a much wider range covering several orders of magnitude, with transitions from the higher vibrational states becoming comparable to the pure rotational transitions of Figure 2.

While we are unaware of any existing experimental data for He–HD inelastic collisions, the current results can be assessed by comparing to the previous calculations. Rotational transitions for $v = 0$ have been computed by Schaefer (1990) and Roueff & Zeippen (1999) which were found to be in good agreement. Our rotational transitions are also found to agree with the previous work. As mentioned above, Roueff & Zeippen (2000) extended their earlier work to include rovibrational transitions, though

limited to $v \leqslant 3$ and $T = 300$–$1000 \, \text{K}$. Therefore, focusing on vibrational transitions, Figure 4 compares the present results for $\{v = 1, j = 1\} \rightarrow \{v' = 0, j'\}$ with those of Roueff & Zeippen (2000). The agreement is fair, with a maximum discrepancy of about a factor of two for the case of $j' = 8$. When we compare results for the highest common initial vibrational level, $v = 3$, the agreement is less satisfactory. Comparing the results in Figure 5 for $\{v = 3, j = 1\} \rightarrow \{v' = 2, j'\}$, we find an order of magnitude difference. The main source of this discrepancy appears to lie in the difference in the respective basis set sizes, as our calculations utilized a basis set of at least a factor of two larger for all energies. As Roueff & Zeippen included no basis states with $v > 3$, we should expect the accuracy of their results to diminish for higher initial vibrational levels. Moreover, in addition to our use of at least twice as many potential expansion terms, we suspect another source of the discrepancy to lie in the fact that Roueff & Zeippen used the harmonic oscillator (HO) approximation for the HD vibrational wave functions in determining the potential matrix element $y_\lambda(vj, v'j'|R)$, whereas in the current work, as mentioned above, numerically determined wave functions for the actual HD interaction potential are adopted. It is expected that agreement should deteriorate for higher v, as the harmonic approximation becomes increasingly invalid. It has been pointed out by Forrey et al. (1997) and Balakrishnan et al. (1999) that, for transitions involving $v \geqslant 2$, the two methods may yield widely discrepant values.

To test this hypothesis and to further explore the discrepancy with the earlier work of Roueff & Zeippen (2000), we plot in Figure 6 a selection of $y_\lambda(vj, v'j'|R)$ for a range of λ using the MR potential and for both numerical and HO wave functions. Figure 6(a) displays matrix elements for $v = v' = 3$, $j = j' = 1$ where it is seen that those based on HO wave functions are shifted to smaller R compared to matrix elements
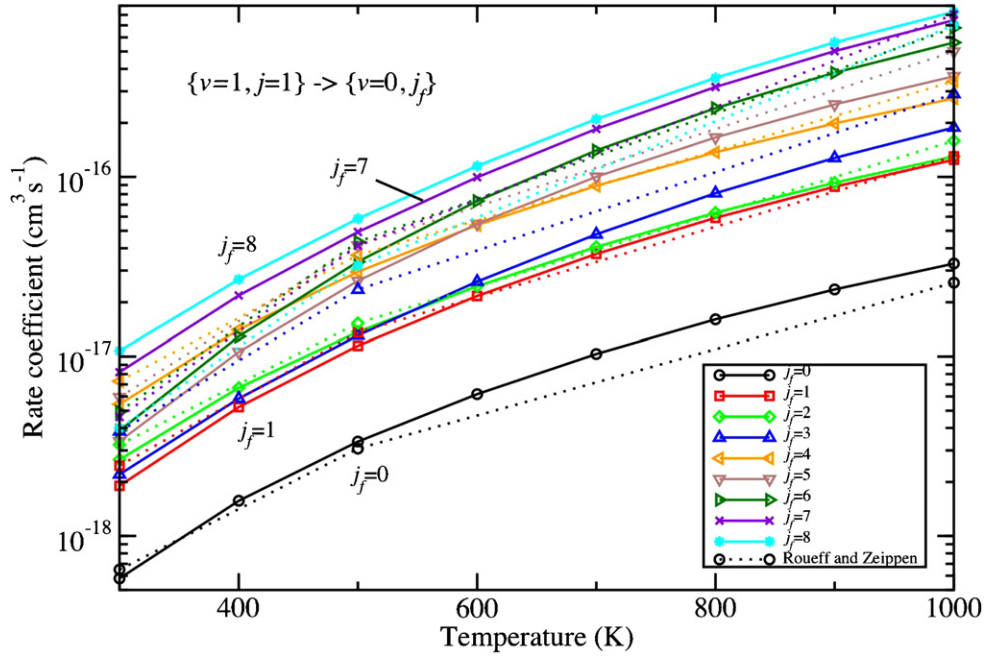
Figure 4. Comparison of He–HD inelastic rate coefficients for $\{v = 1, j = 1\} \rightarrow \{v' = 0, j'\}$: current results, solid lines with symbols; Roueff & Zeippen (2000), dotted lines with same symbols.

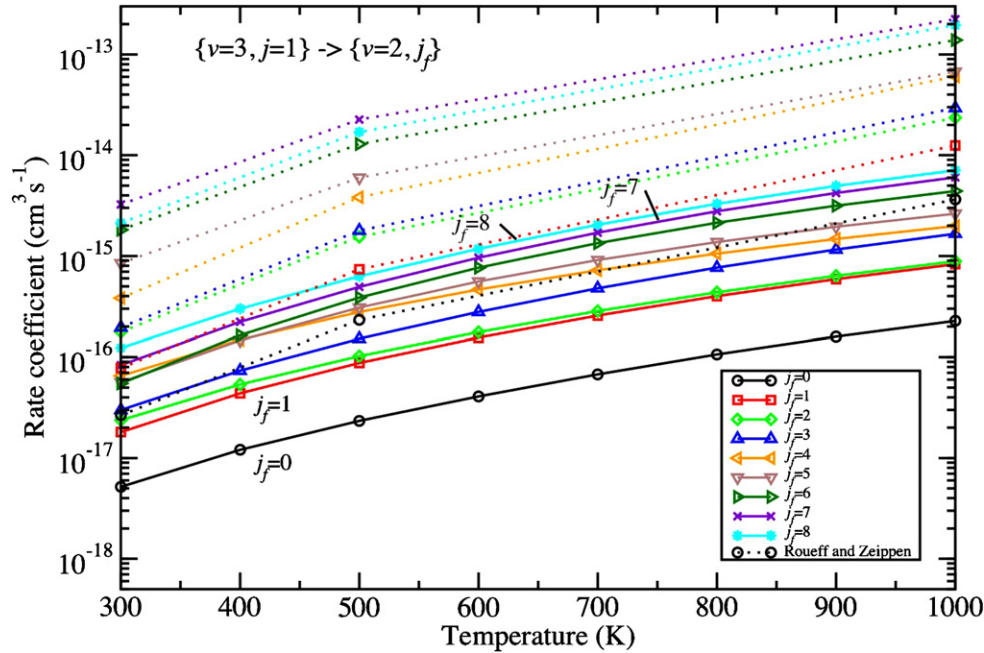(A color version of this figure is available in the online journal.)

Figure 5. Comparison of He–HD inelastic rate coefficients for $\{v = 3, j = 1\} \rightarrow \{v' = 2, j'\}$: current results, solid lines with symbols; Roueff & Zeippen (2000), dotted lines with same symbols.

(A color version of this figure is available in the online journal.)

utilizing wave functions obtained on an anharmonic potential. The difference is more dramatic for $v = v' = 10$, $j = j' = 0$ as displayed in Figure 6(b). Figures 6(c) and (d) display off-diagonal matrix elements corresponding to the initial and final states of Figure 5. Significant differences are again evident between matrix elements obtained with HO and anharmonic wave functions which may partially explain the discrepancies in the rate coefficients given in Figure 5. Further, we note that the matrix elements displayed here are similar to those given for He–H$_2$ in Lee et al. (2005).

Finally, the accuracy of inelastic rate coefficients is sensitive to the details of the PES. Lee et al. (2005) found that the MR potential gives total quenching rate coefficients for $v, j = 1, 0$ in excellent agreement with experiment for He–H$_2$. However, we are unaware of any measurements for $v \geqslant 2$. Unfortunately, the MR PES is only constrained by explicit ab initio energy data for H–H stretching distances of $r = 1.2$–1.6 a.u. For larger r, MR adopted a physically reasonable extrapolation function, but which may lead to some uncertainty in resulting collisional parameters for highly excited v or j levels. Mack
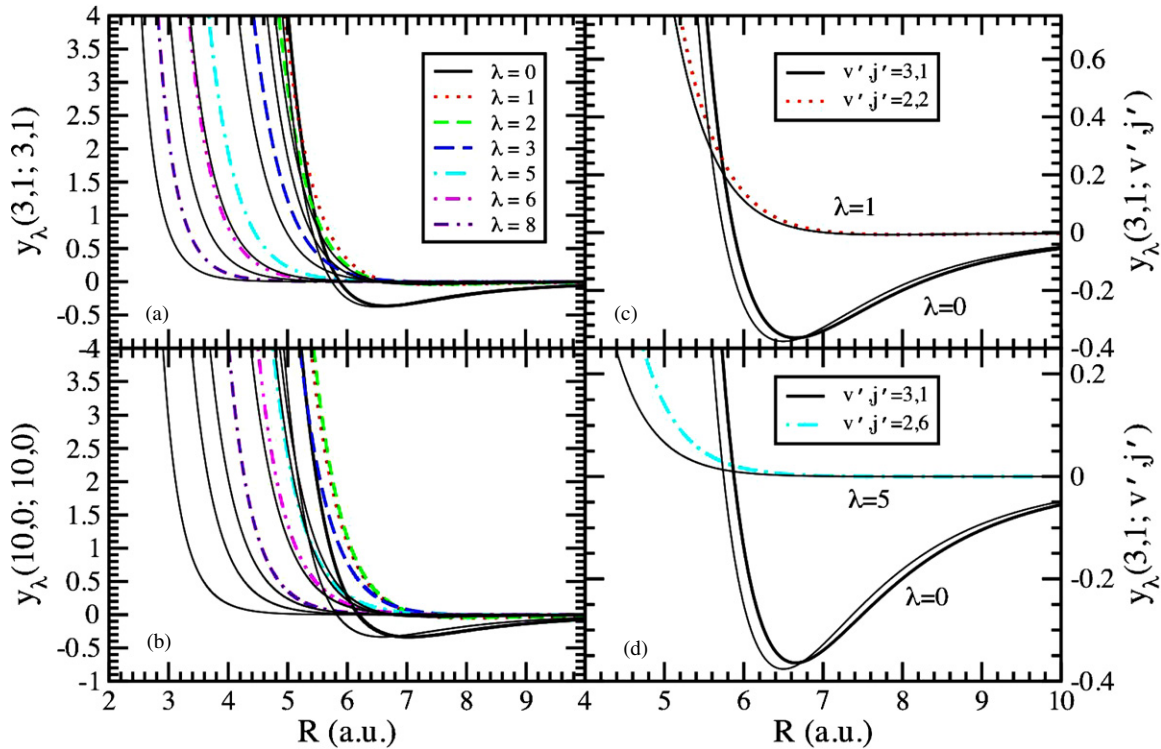
Figure 6. Comparison of interaction potential matrix elements $y_\lambda(vj, v'j'|R)$ (10^{-4} a.u.) as given by Equation (3) using numerical rovibrational wave functions and harmonic oscillator (HO) wave functions. All HO results are given by thin solid black lines. (a) Diagonal elements for v, $j = 3, 1$. (b) Same as (a), but for v, $j = 10, 0$. (c) and (d) Off-diagonal elements for $\lambda = 1$ and $\lambda = 5$, respectively, compared to isotropic diagonal elements. All matrix elements are taken as positive values for plotting convenience.

(A color version of this figure is available in the online journal.)

et al. (2006) explored variations in the large-r extrapolation of the MR surface for He–H$_2$ inelastic rate coefficients for highly excited rovibrational levels near dissociation, but found only small differences. More recently, Paolini et al. (2011) computed the total three-body recombination rate coefficient for H–H–He collisions with the MR surface and found a 25% difference with experiment below 300 K. Agreement with experiment could be obtained with some modification to the large-r part of the MR potential. As the three-body recombination rate is dominated by transitions to highly excited H$_2$ bound and quasi-bound levels, this is a particularly sensitive, though not unique, test of the large-r behavior. Taken together, these observations suggest that the current inelastic rate coefficients for He–HD are uncertain by about 25% for the dominant transitions, while uncertainties for transitions with small rate coefficients are likely larger.

4. ASTROPHYSICAL IMPLICATIONS

A major motivation for this work as outlined in the Introduction is the possible importance of HD as a coolant during the formation of the first stars, so-called Population III stars, from the primordial gas. Here, we have focused on collisions due to He, but H and H$_2$ are also important impactors. In fact, most modeling studies of primordial gas collapse have adopted the H–HD cooling function of Galli & Palla (1998), which was actually obtained by mass-scaling the He–HD $\{v = 0, j = 0\} \rightarrow \{v' = 0, j' = 1\}$ rotational excitation rate coefficients of Schaefer (1990). More elaborate cooling functions have been constructed by Flower et al. (2000) and Lipovka et al. (2005) with the former considering H, He,

and H$_2$ colliders, but the latter limited to H (see the summary in Glover & Abel 2008).

While it is beyond the scope of this work to create an HD cooling function, the new rotational transition rate coefficients will likely have only a minor impact if included in new cooling function computations for T between $\sim$100 and $\sim$1000 K (100 K being the lowest temperature considered by Roueff & Zeippen 2000). However, for $T < 100$ K, Flower et al. (2000) used an extrapolated fit which could now be replaced by our explicit calculations which we note display an upturn in the rate coefficients near 10–50 K. This is potentially significant as HD is expected to be the dominant coolant below $\sim$150 K. On the other hand, the higher temperature portion of the HD cooling function will be modified and improved given our larger range of v and our use of larger basis sets and numerical HD rovibrational wave functions which result in a reduction in the rate coefficient magnitudes compared to the earlier calculations of Roueff & Zeippen (2000), as shown in Figure 5. Lipovka et al. (2005) found that inclusion of rovibrational quenching rates for $v = 1$–3 had a significant impact on the cooling function for $T > 1000$ K and for all densities.

While the possible importance of HD in collapsing primordial clouds may have been first suggested by Varshalovich & Khersonskii (1976), its significance as a coolant is still being debated today (see, for example, Glover & Abel 2008; Wolcott-Green & Haiman 2011). Nevertheless, knowledge of collisional excitation rates is vital to the interpretation of observational data and for application to other environments. In fact, Dalgarno & Wright (1972) proposed that the pure rotational lines of HD and H$_2$ could be used to infer the deuterium abundance if the lines could be measured in nearby molecular clouds. They

even hinted at the role of HD as a coolant in the "prestellar era." Subsequently, pure HD rotational transitions have been observed with the *Infrared Space Observatory* by Bertoldi et al. (1999) and Wright et al. (1999), who detected the $v = 0$, $j = 6 \rightarrow 5$ (or $R(5)$) line and the $v = 0$, $j = 1 \rightarrow 0$ ($R(0)$) line, respectively, toward Orion Peak 1. Neufeld et al. (2006) detected the pure rotational $R(3)$ and $R(4)$ transitions with *Spitzer* toward supernova remnant IC 443. They also obtained tentative detections toward the star-forming region GGD 37 and Herbig–Haro objects HH 54 and HH 7 which they use to estimate the interstellar deuterium abundance. Further, the $R(0)$ line was detected in absorption toward the far-IR continuum sources Sgr B2 (Polehampton et al. 2002) and W49 (Caux et al. 2002).

With respect to rovibrational transitions, there appears to be a single detection: the $\{v = 1, j = 6\} \rightarrow \{v' = 0, j' = 5\}$ line was observed by Ramsay Howat et al. (2002) toward Orion Peak 1 with the United Kingdom Infrared Telescope. However, as H_2 rovibrational emission lines have been observed from numerous photodissociation regions (PDRs), more HD rovibrational detections are likely given improvements in IR detector technology. In fact, HD chemistry and collisional excitation models have been incorporated into the Meudon PDR code, but so far limited to just rotational transitions (Le Petit et al. 2002, 2006). The availability of a comprehensive set of rovibrational collisional rate coefficients, such as begun here, should motivate enhancements in such modeling capabilities.

5. SUMMARY

Collisional rate coefficients of HD are an important ingredient in the simulations of early star formation and interpretations of IR observational data. We have extended the calculations of Roueff & Zeippen (2000) for the He–HD system to include transitions with $j = 0$ and 1 for $v = 0$–17, and for which $\Delta v = 0, -1,$ and -2. The energy and temperature range of the calculations have been expanded into the ultracold limit to resolve resonant features near 0.5 K. While our results generally agree with those of Roueff & Zeippen (2000) for $v \leqslant 2$, we find significant discrepancies for higher vibrational levels. We believe that this is due primarily to differences in the sizes of the basis sets, but also to our use of accurate HD numerical wave functions, as opposed to the harmonic approximation adopted in the previous work. The new He–HD rovibrational collisional rate coefficients should allow for a more accurate treatment of the thermal balance and emission spectra due to HD in a variety of molecular environments.

REFERENCES

Balakrishnan, N., Vieira, M., Babb, J. F., et al. 1999, ApJ, 524, 1122
Bertoldi, F., Timmerman, R., Rosenthal, D., Drapatz, S., & Wright, C. M. 1999, A&A, 346, 267
Boothroyd, A. I., Martin, P. G., & Peterson, M. R. 2003, J. Chem. Phys., 119, 3187
Caux, E., Ceccarelli, C., Pagani, L., et al. 2002, A&A, 383, L9
Dabrowski, I., & Herzberg, G. 1976, Can. J. Phys., 54, 525
Dalgarno, A., & Wright, E. L. 1972, ApJ, 174, L49
Flower, D., & Pineau des Fôrets, G. 2001, MNRAS, 323, 672
Flower, D. R. 2000, MNRAS, 318, 875
Flower, D. R. 2007, Molecular Collisions in the Interstellar Medium (2nd ed.; Cambridge: Cambridge Univ. Press)
Flower, D. R., Le Boulot, J., Pineau des Fôrets, G., & Roueff, E. 2000, MNRAS, 314, 753
Forrey, R. C., Balakrishnan, N., Dalgarno, A., & Lepp, S. 1997, ApJ, 489, 1000
Galli, D., & Palla, F. 1998, A&A, 335, 403
Galli, D., & Palla, F. 2002, Planet. Space Sci., 50, 1197
Glover, S. C. O., & Abel, T. 2008, MNRAS, 388, 1627
Hutson, J. M., & Green, S. 1994, MOLSCAT Ver. 14 (Distributed by Collaborative Computational Project 6; Daresbury Laboratory: UK Eng. Phys. Sci. Res. Council)
Lee, T.-G., Rochow, C., Martin, R., et al. 2005, J. Chem. Phys., 122, 024307
Le Petit, F., Nehmé, C., Le Bourlot, J., & Roueff, E. 2006, ApJS, 164, 506
Le Petit, F., Roueff, E., & Le Bourlot, J. 2002, A&A, 390, 369
Lipovka, A., Núñez-López, R., & Avila-Reese, V. 2005, MNRAS, 361, 850
Machida, M. N., Tomisaka, K., Nakamura, F., & Fujimoto, M. Y. 2005, ApJ, 622, 39
Mack, A., Clark, T. K., Forrey, R. C., et al. 2006, Phys. Rev. A, 74, 052718
McGreer, I. D., & Bryan, G. L. 2008, ApJ, 685, 8
Muchnick, P., & Russek, A. 1994, J. Chem. Phys., 100, 4336
Nagakura, T., & Omukai, K. 2005, MNRAS, 364, 1378
Nakamura, F., & Umemura, M. 2002a, ApJ, 569, 549
Nakamura, F., & Umemura, M. 2002b, Prog. Theor. Phys. Suppl., 147, 99
Neufeld, D. A., Green, J. D., Hollenbach, D. J., et al. 2006, ApJ, 647, L33
Paolini, S., Ohlinger, L., & Forrey, R. C. 2011, Phys. Rev. A, 83, 042713
Percival, I. C., & Seaton, M. J. 1957, Proc. Camb. Phil. Soc., 53, 654
Polehampton, E. T., Baluteau, J.-P., Ceccarelli, C., Swinyard, B. M., & Caux, E. 2002, A&A, 388, L44
Puy, D., Alecian, G., Le Bourlot, J., Léorat, J., & Pineau des Forêts, G. 1993, A&A, 267, 337
Puy, D., & Signore, M. 1997, New Astron., 2, 299
Ramsay Howat, S. K., Timmerman, R., Geballe, T. R., Bertoldi, F., & Mountain, C. M. 2002, ApJ, 566, 905
Roueff, E., & Zeippen, C. J. 1999, A&A, 343, 1005
Roueff, E., & Zeippen, C. J. 2000, A&AS, 142, 475
Schaefer, J. 1990, A&AS, 85, 1101
Schwenke, D. W. 1988, J. Chem. Phys., 89, 2076
Stancil, P. C., Lepp, S., & Dalgarno, A. 1998, ApJ, 509, 1
Uehara, H., & Inutsuka, S.-I. 2000, ApJ, 531, L91
Varshalovich, D. A., & Khersonskii, V. K. 1976, Sov. Astron. Lett., 2, 227
Wolcott-Green, J., & Haiman, Z. 2011, MNRAS, 412, 2603
Wright, C. M., van Dishoeck, E. F., Cox, P., Sidher, S. D., & Kessler, M. F. 1999, ApJ, 515, L29
Zhang, Y. P., Cheng, C. H., Kim, J. T., Stanojevic, J., & Eyler, E. E. 2004, Phys. Rev. Lett., 92, 203003